



Molecular species composition of polar lipids from two microalgae *Nitzschia palea* and *Scenedesmus costatus* using HPLC-ESI-MS/MS

Nicolas Mazzella, Mariem Fadhlaoui, Aurélie Moreira, Soizic Morin

► To cite this version:

Nicolas Mazzella, Mariem Fadhlaoui, Aurélie Moreira, Soizic Morin. Molecular species composition of polar lipids from two microalgae *Nitzschia palea* and *Scenedesmus costatus* using HPLC-ESI-MS/MS. 2023. hal-04173355

HAL Id: hal-04173355

<https://hal.inrae.fr/hal-04173355>

Preprint submitted on 31 Jul 2023

HAL is a multi-disciplinary open access archive for the deposit and dissemination of scientific research documents, whether they are published or not. The documents may come from teaching and research institutions in France or abroad, or from public or private research centers.

L'archive ouverte pluridisciplinaire **HAL**, est destinée au dépôt et à la diffusion de documents scientifiques de niveau recherche, publiés ou non, émanant des établissements d'enseignement et de recherche français ou étrangers, des laboratoires publics ou privés.



Distributed under a Creative Commons Attribution - NonCommercial 4.0 International License

Molecular species composition of polar lipids from two microalgae *Nitzschia palea* and *Scenedesmus costatus* using HPLC-ESI-MS/MS

Nicolas Mazzella¹, Mariem Fadhlou², Aurélie Moreira¹, Soizic Morin¹

¹INRAE Nouvelle-Aquitaine Bordeaux, UR EABX, 50 avenue de Verdun, 33612 Cestas, France

² INRS-ETE, 490 rue de la Couronne, Québec, QC G1K 9A9, Canada

*corresponding author: nicolas.mazzella@inrae.fr

Abstract

This work reports the polar lipid profiles of two freshwater algae: the diatom *Nitzschia palea*, widespread alga that typically inhabits freshwater ponds and rivers, and the *Scenedesmus costatus*, a common green alga. HILIC-ESI-MS/MS analysis was used to determine and quantify the major phospholipids and glycolipids, and their relative molecular species, extracted from the two microalgal cultures. Glycolipids were eluted first, followed by phospholipids partially co-eluting with the sulfoglycolipids. We also studied the fragmentation pattern in the negative ionization mode for galactolipids. The most intense product ion corresponded to the fatty acyl chain located at the *sn*-2 position, which allowed us to determine the stereospecific distribution of the following fatty acids on the glycerol backbone. For green algae, 18:3 fatty acid was frequently occurring in both phospholipids and galactolipids. We also found 16:4 in some molecular species of mono- and digalactosyldiacylglycerol (MGDG and DGDG). The most abundant and characteristic molecular species of MGDG in green algae exhibited the combination (18:3/16:4), whereas DGDG was more saturated than MGDG and contained mainly 18:1, 18:2, or 18:3 at *sn*-1 and shorter acyls like 16:0, 16:1, 16:2, and 16:3 at *sn*-2. It is also remarkable that in the diatom, the phospholipids contained mainly molecular species with saturated or monounsaturated fatty acids such as 16:0, 16:1 and 18:1. In contrast, MGDG and DGDG contained a higher proportion of polyunsaturated fatty acids, such as the unique and abundant MGDG (20:5/20:2).

Introduction

In rivers, periphytic microalgae (i.e. attached to any substrate, either mineral or organic) are often at the basis of the trophic chain, and plays an important resource for higher trophic level taxa. They generally live under a biofilm cohesive form, where organisms from several kingdoms cohabit: besides microalgae, bacteria, fungi and pluricellular micro-eukaryotes are embedded together in a matrix of extracellular polymeric substances. Many herbivores consume biofilms as a primary food source and biofilms, or more specifically their algal component, are receiving increasing attention because they are a source of essential fatty acids for higher consumers ¹⁻². Then, they can be used to describe relationships within the aquatic foodweb ³ and are often used as indicators of trophic quality in ecosystems. It has long been shown that total fatty acid profiles differ between groups of algae. In freshwater biofilms, which are often dominated by diatoms and chlorophytes, the specific distribution influences the overall composition of the food available for consumers, making it a crucial driver of the health and stability of aquatic food chains. According to Arts et al. ⁴, both ω 3 eicosapentaenoic acid (EPA, 20:5*n*-3) and docosahexaenoic acid (DHA, 22:6), and the ω 6 arachidonic acid (ARA, 20:4*n*-6) are key fatty acids for zooplankton and fish. Freshwater diatoms are also rich in palmitoleic acid (16:1*n*-7), palmitic acid (16:0), and myristic acid (14:0). Most importantly, diatoms are an important source of fatty acids essential for higher

consumers, especially EPA and ARA ¹, and also contain low but significant amounts of DHA ⁵. In contrast, the major fatty acids in chlorophytes are α -linolenic acid (ALA, 18:3*n*-3), palmitic acid, oleic acid (18:1*n*-9), and α -linoleic acid (LIN, 18:2*n*-6). Lastly, phosphatidylglycerol and some peculiar galactolipids are the main component of thylakoid membranes in all microalgae ⁶⁻⁸, and especially their respective fatty acid constituent (i.e. molecular species) were partly investigated for diatom and chlorophyte species so far. Actually, with the exception of a few marine species, lipid algal metabolism has been little studied to date, and we still have limited knowledge of the biochemical processes underlying the synthesis or plasticity of the major lipid classes ⁹⁻¹⁰.

This is within this framework that we are interested in the analysis of polar lipids of two freshwater microalgae (*Nitzschia palea* and *Scenedesmus costatus*). On the one hand, we aim to characterize the main molecular species associated with both glycolipids and phospholipids, including some fragmentation patterns in mass spectrometry. On the other hand, we aim to quantify each of these compounds. The aim is here to provide a methodology, and then to enlighten the typical polar lipidome profile for both “model” diatom and green algae.

Experimental

Chemicals and materials

The following polar lipid standards were purchased from Avanti Polar Lipids: 1-palmitoyl-2-oleoyl-*sn*-glycero-3-phosphocholine or PC (16:0/18:1) (850457), 1-palmitoyl-2-oleoyl-*sn*-glycero-3-phosphoethanolamine or PE (16:0/18:1) (850757), 1-palmitoyl-2-oleoyl-*sn*-glycero-3-phospho-(1'-rac-glycerol) or PG (16:0/18:1) (840457), 1,2-diheptadecanoyl-*sn*-glycero-3-phosphocholine or PC (17:0/17:0) (850360), 1,2-diheptadecanoyl-*sn*-glycero-3-phosphoethanolamine or PE (17:0/17:0) (830756), 1,2-dipentadecanoyl-*sn*-glycero-3-phosphoethanolamine or PE (15:0/15:0) (850704), and 1,2-diheptadecanoyl-*sn*-glycero-3-phospho-(1'-rac-glycerol) or PG (17:0/17:0) (830456), L- α -phosphatidylserine (Soy, 99%) (sodium salt) (870336) for the phospholipid standards, and monogalactosyldiacylglycerol (840523), digalactosyldiacylglycerol (840524) and sulfoquinovosyldiacylglycerol (840525) from plant extracts as glycolipid standards. Ammonium acetate (LiChropur) were provided by Sigma-Aldrich. Acetonitrile, methanol (MeOH) tert-Butyl methyl ether (MTBE) and isopropanol HPLC grades were purchased from Biosolve Chimie, France. Ultrapure water (UPW) was obtained from Direct-Q® Water Purification System (Merck Millipore).

Algal cultures

The algal cultures were purchased at the Thonon Culture Collection ¹¹ under culture references TCC 583 (*i.e.* the diatom *Nitzschia palea*) and TCC 744 (*i.e.* the chlorophyte *Scenedesmus costatus*). Both taxa were selected to be common microalgal species in freshwater environments, originated from rivers of the French metropolitan territory. Indeed, the diatom was isolated from the river la Chiers at Longlaville (Eastern France), and the chlorophyte from the stream Foron, a tributary of Lake Léman (France/Switzerland). The algal cultures were incubated in thermoregulated chambers (temperature: 18°C, light:dark cycle: 16 h:8 h, Photosynthetic Active Radiation reaching the cultures under light conditions: 65 $\mu\text{mol photons}\cdot\text{sec}^{-1}$), in 100-mL erlenmeyers for 2 exponential growth cycles of 7 days before the experiment began. After the two growth cycles aiming at acclimating and synchronizing the cultures, 10 mL of diatom culture (*N. palea*) were put into 60 mL of modified Dauta medium ¹² to reach an initial cell density of $297\pm75 \text{ cell}\cdot\mu\text{L}^{-1}$. Five replicate cultures were prepared and placed in the thermoregulated chambers under the conditions described above for pre-exposure. In the case of the chlorophyte *S. costatus*, 20 mL of culture and 50 mL of modified Dauta medium (Dauta, A. 1982.) were used to obtain an initial cell density of $1834\pm144 \text{ cell}\cdot\mu\text{L}^{-1}$. Cultures were performed in five independent replicates as

well, in the thermoregulated chambers under the same conditions as *N. palea*.

Lipid extraction

Briefly, 150 mg of microbeads (0.5 mm diameter) were added in 2 mL microtubes, as well as 10-20 mg (dry mass) of a microalgae cultures weighed using a Mettler Toledo NS204S precision balance. 50 μL of solution of PE (15:0/15:0) at 100 $\text{ng}\cdot\mu\text{L}^{-1}$ was added as surrogate, prior to extraction. The extraction was adapted from Matyash et al.¹³, it consists in the initial addition of 1 mL a MTBE:MeOH (3:1, v/v) mixture, and 650 μL of an UPW:MeOH (3:1, v/v) mixture. The use of the MP Biomedicals FastPrep-24 5G (3 cycles of 15 s) allowed homogenization of the solution as well as mechanical lysis of the sample via the microbeads, and thus release of analytes from within the sample. A centrifugation at 12 000 RPM (i.e. 16 000 g) allowed separation of upper lipophilic phase (MTBE) from lower hydrophilic phase (UPW and MeOH). At this stage 600 μL of the lipophilic phase was collected. A second extraction (3 cycles 15 s) step was carried out after addition of 700 μL of MTBE:MeOH mixture 3:1 (v/v) and 455 μL UPW:MeOH mixture 3:1 (v/v) to residual hydrophilic phases. After centrifugation, the supernatant was collected and added to previous one. Only organic lipophilic phases (i.e 1.1 mL) was kept for further polar lipid analysis. The whole procedure was performed on ice to avoid any enzymatic activities that could lead to a possible alteration of lipid extracts and butylated hydroxytoluene (BHT, 0.01% (w/v)) was initially added as antioxidant.

Extracts obtained stored in freezer at -80°C . In addition to samples, solvent alone as procedural blank was extracted in order check the absence of any contamination during extracting step. Prior to HILIC-ESI-MS/MS analysis, 50 μL of internal standards (i.e. PC, PG and PE (17:0/17:0)) at a concentration of 33.3 $\text{ng}\cdot\mu\text{L}^{-1}$ were added to the sample. MTBE was evaporated with a gentle stream of N_2 , and then diluted in appropriate volume (typically 250 to 1000 μL) of isopropanol. The sample can be kept at -18°C , at least 1 week, until injection.

HILIC-ESI-MS/MS analysis

Lipid extracts were analyzed with a Dionex Ultimate 3000 HPLC (Thermo Fisher Scientific, France). An API 2000 triple quadrupole mass spectrometer (Sciex, France) was used for detection. Chromatographic separation of both glycolipids and phospholipids was performed on a Luna NH_2 HILIC (3 μm , 100×2 mm) with a Security Guard cartridge NH_2 (4×2.0 mm). The injection volume and temperature column were set to 20 μL and 40°C , respectively. The chromatographic separation conditions were reported in Table S 1, a final pH value of 6.8 was retained for the ammonium acetate buffer. Further details on initial method optimization and performances related to phospholipid HILIC separation can be found in Mazzella et al.¹⁴. Quantitation of phosphatidylcholine (PC), phosphatidylethanolamine (PE), phosphatidylglycerol (PG), phosphatidylinositol (PI), and were respectively carried out with:

PC (16:0/18:1), PE (16:0/18:1), PG (16:0/18:1). Quantitation of glycolipids was carried out with MGDG (16:3_18:3) (63 % of the total MGDG standard), DGDG (18:3/18:3) (22 % of the total MGDG standard), and SQDG (34:3) (78 % of the total SQDG standard). The internal standards utilized were PC (17:0/17:0) for PC phospholipids, PE (17:0/17:0) for PE phospholipids and both MGDG and DGDG glycolipids, and PG (17:0/17:0) for PG phospholipids and SQDG glycolipids. Calibrations curves are provided as supplementary information (Fig. S 2). For glycolipids, a quadratic model was used for the data fitting, while a linear regression was generally used for phospholipids. The limits of quantification for phospholipids and glycolipids are provided in Table S 2, they are finally expressed as nmol mg⁻¹ (dry weight) since a typical sample of 10 mg of culture is considered for the initial extraction step. Additionally, PE (15:0/15:0) was used as surrogate for the whole extracting procedure, with a typical recovery of 102±23 % (n=10)¹⁴. The mass spectrometry parameters were reported in Table S 3, and Q1 > Q3 transitions for each molecular species of PC, PG, PE, MGDG, DGDG and SQDG are provided in Table S 4. This HILIC-ESI-MS/MS method was adapted from a previous work¹⁴, however we have here selected the molecular species representative of microalgae, and thus reduced the number of MRM transitions followed during the two acquisition periods (Table S 4). Thus, excepted for SQDG, it was possible to determine for each molecular species searched the *sn*-1/*sn*-2 ratio based on the relative abundances of

the ions corresponding to the two acyl chains.

Phospholipid and glycolipid nomenclatures

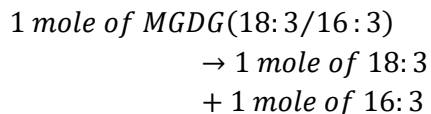
Polar glycerolipids are constituted of a glycerol backbone esterified by two fatty acids on the *sn*-1 and *sn*-2 positions. The moiety linked to the *sn*-3 position refers to the polar head group (e.g., *sn*-phospho-3-glycerol for the PG, a β-D-galactosyl group for MGDG). Each polar head group defines a phospholipid or glycolipid class, and each class can be divided into several molecular species according to the fatty acyl chain composition and distribution. Polar glycerolipids are abbreviated as follows: when the fatty acyl chain structures are resolved but the *sn*-1 and *sn*-2 positions remain unclear, then the phospholipids or glycolipids are designated PL (C:n_C:n), with C referring to the sum of the number of carbon atoms and n to the number of double bonds for each fatty acyl chain. When the acyl chain composition and distribution are known, then the phospholipids are noted as PL (C:n1/C:n2), where C:n1 and C:n2 correspond to the fatty acids linked to *sn*-1 and *sn*-2 positions, respectively [e.g., PG (16:0/18:1) for 1-palmitoyl-2-oleoyl-*sn*-glycero-3-phospho-*rac*-1-glycerol].

Conversion of phospholipids and glycolipids in fatty acid equivalents

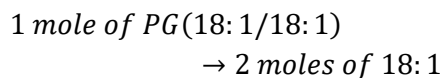
Following the analysis of the different classes of polar lipids, and having

access to the molecular species within each class, it is then possible to deduce the different fatty acids from the acyl chains determined before. To this purpose, each mole of each molecular species was converted into its fatty acid equivalent.

Equation 1



Equation 2



Equation 1 illustrates the case where the acyl chains are asymmetric (i.e. the fatty acid at *sn*-1 is different from that at *sn*-2), while Equation 2 corresponds to the other possible case (i.e. the presence of two fatty acids with both the same numbers of carbons and unsaturations).

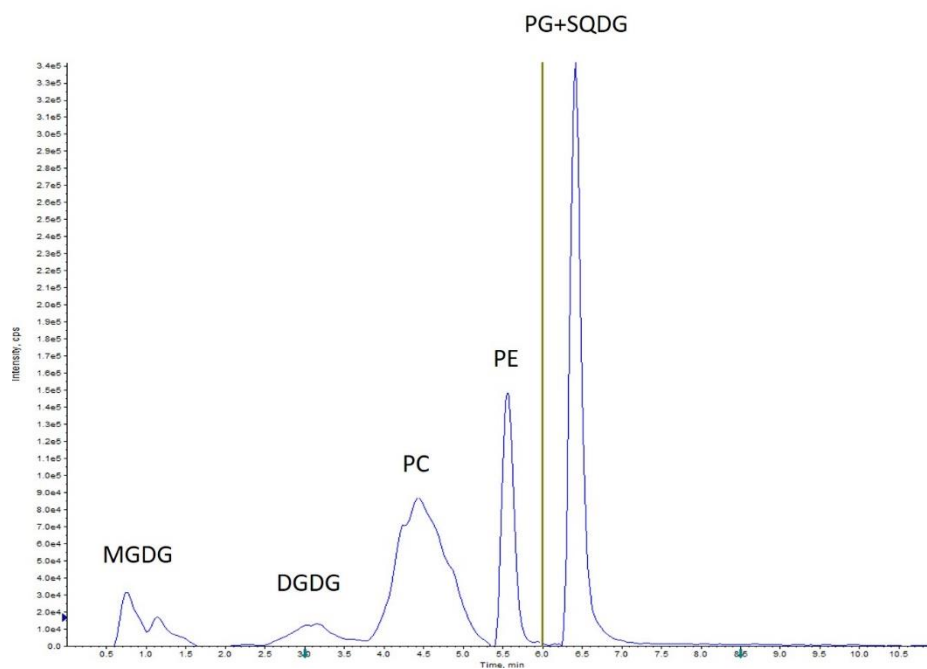


Figure 1. HILIC-ESI-MS/MS analysis of a phospholipid and glycolipids extracted from *S. costatus*.

Results and discussion

In a HILIC-ESI-MS/MS method originally developed for phospholipid analysis¹⁴, it was proceed to the addition of MRM transitions for three classes of glycolipids commonly observed in microalgae¹⁵⁻¹⁷: monogalactosyldiacylglycerol (MGDG), digalactosyldiacylglycerol (DGDG) and sulfoquinovosyldiacylglycerol (SQDG). shows the elution orders for the major phospholipids (PC, PE, and PG), as well as the main glycolipids (MGDG, DGDG, and SQDG) obtained from the green algal culture extract. MGDG was eluted first in our conditions, followed by the DGDG around 3.1 min. Finally, it was SQDG that was co-eluted with PG at 6.4 min (Table S 2).

A first screening of both *N. palea* and *S. costatus* extracts for five phospholipid classes, as well as all the possible related molecular species¹⁴, revealed the absence of any quantifiable amount of phosphatidylinositol (PI) or phosphatidylserine (PS). This result appeared as consistent, since PI, with both PC and PE, is mainly observed in dinoflagellates like *Schizochytrium* sp¹⁸. Afterwards, in addition to the observation obtained with our initial screening¹⁴ for both *S. costatus* and *N. palea*, the number of MRM transitions simultaneously followed per compound was reduced (Table S 4). Actually, these transitions have been selected with respect to the molecular species expected for various microalgae

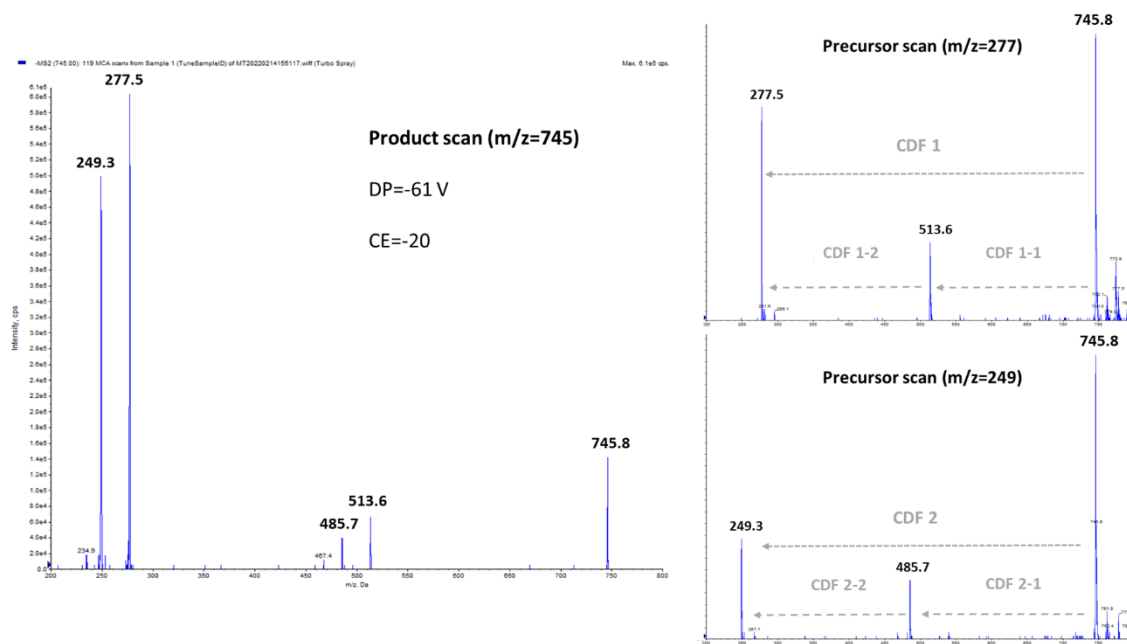


Figure 2. Negative ionization and collision-induced dissociation of MGDG (18:3/16:3), with either product scanning from m/z 745.8 (left part) or precursor scanning for m/z 277.5 and m/z 249.3 ions (right part).

(green algae, cyanobacteria, and diatoms), as well as those reported in several previous studies involving lipidomics^{14-16, 19-22}. With the exception of SQDG, this enabled the consideration of two MRM transitions for

each analyte and provided here access to the determination of the *sn*-1 and *sn*-2 locations of the acyl chains. However, in order to consider the different MRM transitions associated with each molecular species, it was necessary to determine the likely fragmentation obtained in negative electrospray ionization for such glycolipids.

MGDG fragmentation pathways

Low-energy collisionally activated dissociation with tandem quadrupole mass spectrometry previously allowed structural characterization of glycerophospholipids, especially in negative ionization mode²³. Regarding glyceroglycolipids, some studies have focused on the structural elucidation, and thus the determination of fragmentation pathways from positive electrospray ionization mode²⁴⁻²⁵. In our case, we focused more precisely on the negative ionization, and the subsequent fragmentation, obtained from a monogalactosyldiacylglycerol standard like MGDG (18:3/16:3) (the fragmentation of DGDG molecular species, not showed here, being similar). The left part of Figure 2 exhibited the fragments obtained in product scan mode from m/z 745.8, which corresponds to MGDG (18:3/16:3), as a deprotonated molecule $[M-H]^-$, while the right parts correspond to the precursors determined from the product ions m/z 277.5 and 249.3. Herrero et al.²⁶ have previously observed fragments with m/z 277 ratio, and it was attributed to γ -linolenic acid (18:3n-6) from a MGDG molecular species in their study. It should be noted that in the case of

HPLC-MS/MS analyses, the m/z 277 ratio corresponds more generally to any deprotonated 18:3 isomers.

In order to explain these observations, it can be assumed, as for phospholipids during a negative ionization mode, mechanisms like charge-driven fragmentation (CDF) processes would occur²⁷. Due to the intensity of the two carboxylate ions at m/z 249.3 and m/z 277.5 formed from the parent ion at m/z 745.8 (Figure 2), a CDF-type mechanism is mainly suspected. In Figure 3, we proposed two possible pathways with a CDF 1 mechanism inducing the formation of the R_1COO^- ion characterized by a m/z 277.5 ratio, and then another CDF 2 mechanism resulting in the formation of the R_1COO^- ion characterized by a m/z 249.3 ratio. The predominance of these two CDF mechanisms being confirmed by the precursor scanning with the observation of the prevailing m/z 745.8 ratio, corresponding to the pseudo-molecular ion $[M-H]^-$.

In our case, a likely second mechanism could also be taken into account with an initial neutral loss of the fatty acyl chain as a ketene (i.e. $R_2CH=C=O$) from *sn*-2 position (CDF 1-1). It can be proposed that the deprotonation at the α carbon on the acyl chain affords an 'enolate' ion²⁸ that immediately undergoes a C-O bond releasing the $C_{14}H_{23}-CH=C=O$ neutral, and then affording m/z 513.6 (Figure 4) ion with a negatively charged oxygen atom (i.e. alkoxide ion). A following CDF process (i.e. CDF 1-2) may produce the release of the fatty acyl chain located at *sn*-1 position, with the occurrence of ion at m/z 277.5. The

alternative pathway consists in the neutral loss of fatty acid a ketene (i.e. $R_1CH=C=O$) from *sn*-1 position (CDF 2-1), and then the final formation of the m/z 249.3 ion (CDF 2-2). In the Figure 4, for readability reasons, only a CDF 1-1 pathway, preceding the CDF 1-2 step, with a proton transfer rearrangement was shown. The suggested alternative CDF 2-1 and 2-2 pathways would follow the same principle. Lastly, two other mechanisms might result in the neutral loss of acyl chains as protonated acids (i.e. R_1COOH or R_2COOH). In that case, we should observe ions at m/z 495.5 and m/z 467.5, but these were hardly visible and anyway much less intense than the m/z 513.6 and m/z 485.7 ions for collision energies tested between 10 and 30 eV.

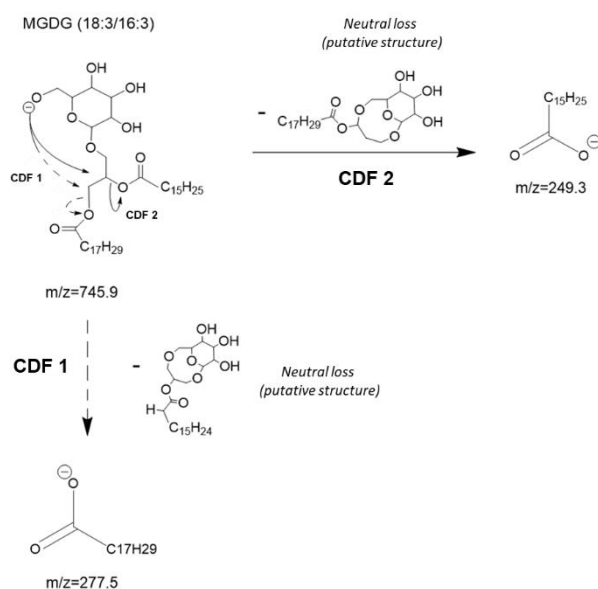


Figure 3. Proposed collision-induced dissociation (CID) pathways of MGDG (18:3/16:3) after electrospray ionization showing the direct formation of $[R_1COO]^-$ and $[R_2COO]^-$ ions via CDF 1 and 2 processes, respectively.

In this study, whatever the mechanisms and pathways involved, it appears that the most intense product ion corresponds to the fatty acyl chain located at *sn*-1 position, allowing the determination of stereospecific distribution of subsequent fatty acids on the glycerol backbone. Such a result come into sight as inverted in comparison to the usual negative fragmentation and the latterly observed *sn*-1/*sn*-2 ratio for phosphatidylglycerol, and other phospholipids in general^{23, 29-33}. Such a property has been employed here in order to determine the likely regiochemistry of the two acyl chains within the molecular species of MGDG and DGDG, in addition to those associated with PG, PE and PC. This is illustrated by ion ratios observed for the three pairs of molecular species (i.e. possible isomers) of PG (16:0/16:1) and PG (16:1/16:0), PE (16:1/18:1) and PE (18:1/16:1), and DGDG (20:5/16:1) and DGDG (16:1/20:5) (Fig. S1). For instance, the higher intensity of the m/z 253 ratio over the m/z 255 ratio, both obtained from the m/z 719 ion, indicates the preferential occurrence of the PG (16:0/16:1) regioisomer in that case. Conversely, the higher intensity of the m/z 301 ratio over the m/z 253 ratio, both originating from the m/z 935 ion, should mainly correspond to the DGDG (20:5/16:1) conformation.

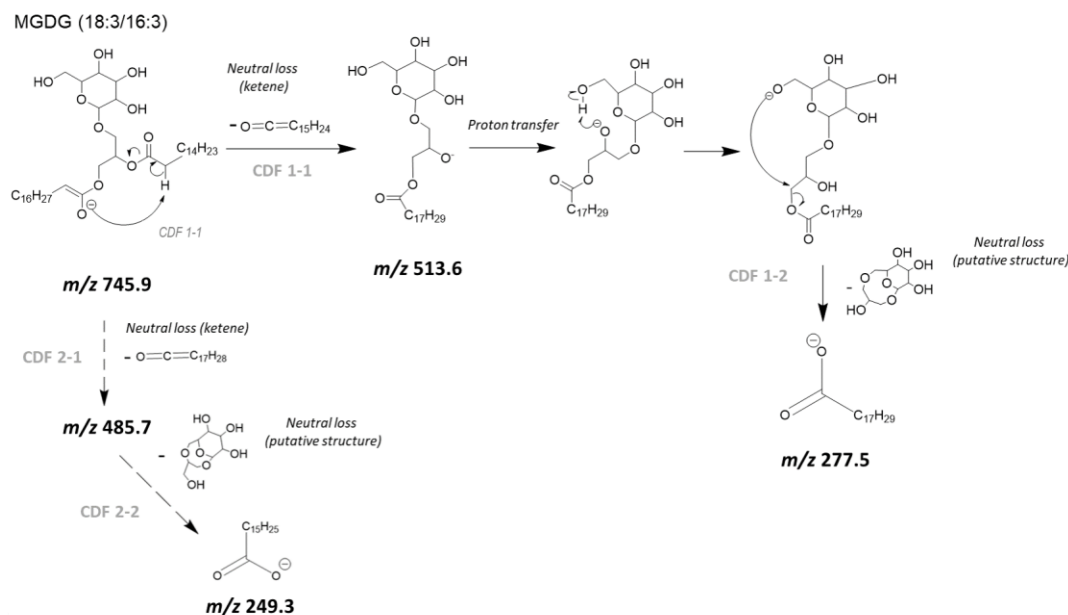


Figure 4. Proposed collision-induced dissociation (CID) pathways of MGDG (18:3/16:3) after electrospray ionization showing the likely successive formation of $[M - H - R_2CH=C=O]^-$ and $[R_1COO]^-$ ions (CDF 2-1, and then CDF 2-2 processes) or $[M - H - R_1CH=C=O]^-$ and $[R_2-COO]^-$ ions (CDF 1-1, and then CDF 1-2 processes).

Intact polar lipids of two microalgae extracts

Phospholipid and glycolipid molecular species of *N. palea* and *S. costatus*.

The upper parts of the Table 1 and Table 2 plot for the two microalgae the different molecular species within the detected phospholipids (PE, PG and PC), as well as among the two galactolipids (MGDG and DGDG). In the case of SQDG, fragmentation in negative mode mainly allowed the observation of the characteristic ion at m/z 225^{23, 34}, and not the couple of ions associated with losses of acyl chains. The expected neutral loss³⁵ (e.g. m/z 537.4 with a precursor ion m/z 793.5 corresponding to the neutral loss of a 16:0 fatty acid) was barely

visible in our case, regardless of the collision energy applied. It was therefore not possible in this case, unlike the other glycerolipids investigated here, to determine the fatty acid composition, resulting in a general SQDG-type notation ($\Sigma C:\Sigma n$), with ΣC the total number of carbon and Σn the total number of double bonds of the two fatty acids, respectively. Within the phospholipids of *N. palea* (Table 1), it is remarkable that PE and PG contain mainly molecular species with saturated (SFAs) or monounsaturated (MUFAs) fatty acids like 16:0, 16:1, and 18:1. PC differs with many more polyunsaturated fatty acids (PUFAs) such as 20:5 and 22:6. This is also the case for MGDG and DGDG, with the observation of the unique and very abundant MGDG

(20:5/20:2) with nearly 2.66 nmol mg⁻¹, followed by the four molecular species of DGDG of which three contain 20:5. In accordance with the description in other previous works compounds ^{9, 19, 21}, it should be noted that fatty acids with 16 carbons along with PUFAs, when present, are preferentially positioned in *sn*-2 in this study, reflecting the prokaryotic pathway in the original synthesis of these acylglycerol lipids. Finally, the predominant species of SQDG (32:1) probably corresponds to a combination of 16:0 and 16:1, although this cannot be confirmed analytically due to specific CID fragmentation in our case, as mentioned above.

As reported in Table 2, concerning the green algae (*S. costatus*), we note, unlike the diatom strain, the frequent presence of 18:3, both among phospholipids and galactolipids, while 20:5 is absent this time. We also find some 16:4 in some molecular species of both MGDG and DGDG. The characteristic MGDG species in most green algae are actually (18:3/16:4), and to a less amount (18:3/16:3), which may be produced by sequential desaturation of MGDG (18:1/16:0) as shown for *Chlamydomonas* or *Dunaliella* ³⁶⁻³⁷. DGDG are somewhat more saturated than MGDG, and contains mainly 18:1, 18:2

or 18:3 at *sn*-1 and the shorter 16:0, 16:1, 16:2 and 16:3 moieties at *sn*-2. In addition, the preferential occurrence of 16:3 and 16:4 over 18:3 PUFAs in DGDG compared to PE, PC and PG molecular species was also revealed by lipid content and fatty acid composition of the green alga *Scenedesmus obliquus*³⁸ determined with different methodology and analytical techniques (i.e. thin layer and gas liquid chromatography). Consequently, our results appeared to be consistent with these general patterns reported for some *Chlorophyceae*.

Besides, in the case of PG, MGDG and DGDG, when a PUFA is associated with either a MUFA or SFA, it is then mostly found in the *sn*-1 position. The opposite pattern appeared for PE and PC, indicating a likely biosynthesis in the endoplasmic reticulum for these two phospholipids ²¹.

Table 1. Amounts of phospholipid and glycolipid molecular species extracted from *N. palea* (n=5). Molecular weights and relative standard deviations (RSD) are also indicated.

Molecular species	MW (Da) ^a	Mean (nmol.mg ⁻¹) ^b	SD	%RSD
PE(16:0/16:1)	689	<div><div></div></div> 0.60	0.211	35%
PE(16:1/16:1)	687	<div><div></div></div> 0.76	0.350	46%
PE(18:1/16:1)	715	<div><div></div></div> 0.37	0.148	40%
PG(16:1/14:0)	692	<div><div></div></div> 0.13	0.057	46%
PG(16:0/16:1)	720	<div><div></div></div> 0.56	0.213	38%
PG(16:1/16:1)	718	<div><div></div></div> 0.27	0.098	37%
PG(18:1/16:1)	746	<div><div></div></div> 0.38	0.155	41%
PG(20:5/18:1)	794	<div><div></div></div> 0.10	0.000	0%
PC(20:5/16:1)	778	<div><div></div></div> 0.15	0.125	83%
PC(20:5/22:6)	852	<div><div></div></div> 0.11	0.012	11%
MGDG(20:5/20:2)	828	<div><div></div></div> 2.66	1.417	53%
DGDG(16:1/16:1)	916	<div><div></div></div> 0.13	0.032	24%
DGDG(20:5/16:1)	936	<div><div></div></div> 0.23	0.090	40%
DGDG(20:5/16:2)	934	<div><div></div></div> 0.19	0.097	50%
DGDG(20:5/20:0)	994	<div><div></div></div> 0.15	0.057	38%
SQDG(30:1)	765	<div><div></div></div> 0.06	0.012	20%
SQDG(32:0)	795	<div><div></div></div> 0.08	0.014	17%
SQDG(32:1)	793	<div><div></div></div> 1.15	0.351	31%
SQDG(32:2)	791	<div><div></div></div> 0.16	0.035	22%
SQDG(34:5)	813	<div><div></div></div> 0.06	0.010	17%
SQDG(36:4)	843	<div><div></div></div> 0.05	0.007	14%
SQDG(36:5)	841	<div><div></div></div> 0.13	0.025	19%
SQDG(42:5)	925	<div><div></div></div> 0.05	0.008	15%
Σ PE		<div><div></div></div> 1.73	0.692	40%
Σ PG		<div><div></div></div> 1.43	0.497	35%
Σ PC		<div><div></div></div> 0.26	0.137	53%
Σ MGDG		<div><div></div></div> 2.66	1.417	53%
Σ DGDG		<div><div></div></div> 0.71	0.271	38%
Σ SQDG		<div><div></div></div> 1.74	0.439	25%

^a Average molecular weight.

^b nmol mg⁻¹ of dry weight.

Polar lipid classes of *N. palea* and *S. costatus*. The bottom of Table 1 as well as the bottom of Table 2 summarize the sums of each molecular species, and with these sums, it can be possible to deduce the polar lipid classes for each of the two microalgae. In both cases, MGDG and SQDG are predominant among the glycolipids, followed by PG in the phospholipids from thylakoids. Glycolipids including MGDG, DGDG and SQDG are prevalent in the plant kingdom, representing around 70–85 % of membrane lipids in chloroplasts³⁹. It is well known that thylakoid membrane of chloroplasts is unique in lipid composition, with mono- and digalactosyldiacylglycerol as major constituents. The ratio of bilayer-forming DGDG to non-bilayer-forming MGDG may affect the properties of chloroplast membranes by altering the lipid bilayer from hexagonal II to lamellar phases⁴⁰. SQDG and PG are classified as acidic lipids, with their negative charge at neutral pH. In addition, acidic lipids with negative charge in their head groups also affect the organization of thylakoid membranes. PG is the only phospholipid produced in the chloroplasts and it is usually an essential component in the

center of photosystem II⁴¹. SQDG too has an important function in photosynthesis, although the requirement for this lipid differs among species. PG and SQDG are at least partially functionally redundant, which may be related to maintenance of an anionic charge on the surface of the thylakoid membrane⁴². The amount of phospholipids in microalgae is usually less than that of the glycolipids, with a few exceptions. The main phospholipids are typically phosphatidylcholine, phosphatidylethanolamine, and phosphatidylglycerol. There is a wide variation in the percentages of different found phospholipids in brown algae⁴³⁻⁴⁴, for instance. Furthermore, apart from phosphatidylglycerol, phospholipids are occurring in extraplastidial membranes and among them, phosphatidylcholine and phosphatidylethanolamine are usually the most abundant within algae¹⁵, as observed for *N. palea*.

Table 2. Amounts of phospholipid and glycolipid molecular species extracted from *S. costatus* (n=5). Molecular weights and relative standard deviations (RSD) are also indicated.

Molecular species	MW (Da) ^a	Mean (nmol.mg ⁻¹) ^b	SD	%RSD
PE(18:1/16:1)	715	0.03	0.01	30%
PE(18:1/18:1)	743	0.02	0.01	45%
PE(18:1/18:2)	741	0.07	0.02	30%
PE(18:1/18:3)	739	0.17	0.05	29%
PE(18:2/18:3)	737	0.33	0.11	33%
PE(18:3/18:3)	735	0.22	0.07	31%
PG(16:0/16:0)	722	0.03	0.00	11%
PG(16:1/16:0)	720	0.03	0.00	4%
PG(18:1/16:0)	748	0.63	0.04	6%
PG(18:2/16:0)	746	0.37	0.03	9%
PG(18:3/16:0)	744	0.30	0.01	5%
PG(18:4/16:0)	742	0.01	0.00	4%
PG(16:1/18:1)	746	0.12	0.01	7%
PG(16:1/18:2)	744	0.09	0.01	15%
PG(16:1/18:3)	742	0.31	0.01	5%
PG(18:1/18:1)	774	0.01	0.00	21%
PG(18:1/18:2)	772	0.01	0.00	16%
PG(18:3/18:1)	770	0.01	0.00	9%
PG(18:3/18:2)	768	0.01	0.00	24%
PG(18:3/18:3)	766	0.01	0.00	32%
PC(16:0/18:2)	758	0.01	0.00	9%
PC(16:0/18:3)	756	0.07	0.02	24%
PC(18:1/18:3)	782	0.07	0.02	33%
PC(18:2/18:3)	780	0.23	0.04	18%
MGDG(18:3/16:3)	746	0.15	0.06	41%
MGDG(18:3/16:4)	744	3.17	0.37	12%
DGDG(16:0_18:1) ^c	918	0.09	0.01	11%
DGDG(18:2/16:0)	916	0.08	0.00	1%
DGDG(18:3/16:0)	914	0.13	0.01	6%
DGDG(16:1/18:1)	916	0.10	0.01	15%
DGDG(16:1_18:2) ^c	914	0.08	0.02	22%
DGDG(18:3/16:1)	912	0.18	0.03	18%
DGDG(18:1/16:2)	914	0.06	0.01	8%
DGDG(18:2/16:2)	912	0.08	0.01	13%
DGDG(18:3/16:2)	910	0.18	0.03	19%
DGDG(18:1/16:3)	912	0.07	0.01	18%
DGDG(18:2/16:3)	910	0.12	0.02	19%
DGDG(18:3/16:3)	908	0.31	0.03	9%
DGDG(16:4/18:2)	908	0.02	0.00	18%
DGDG(16:4/18:3)	906	0.20	0.02	12%
DGDG(18:3/18:1)	940	0.02	0.01	70%
DGDG(18:3/18:2)	938	0.07	0.02	32%
DGDG(18:3/18:3)	936	0.13	0.03	22%
SQDG(32:0)	795	0.48	0.12	25%
SQDG(32:1)	793	0.07	0.01	7%
SQDG(34:0)	823	0.06	0.00	9%
SQDG(34:1)	821	0.92	0.13	14%
SQDG(34:2)	819	0.49	0.08	17%
SQDG(34:3)	817	1.38	0.13	9%
SQDG(34:4)	815	0.15	0.00	3%
SQDG(36:1)	849	0.05	0.00	6%
SQDG(36:3)	845	0.06	0.01	13%
SQDG(36:4)	843	0.05	0.01	15%
SQDG(36:6)	839	0.13	0.01	9%
Σ PE		0.84	0.26	31%
Σ PG		1.94	0.11	6%
Σ PC		0.38	0.07	20%
Σ MGDG		3.32	0.42	13%
Σ DGDG		1.96	0.07	3%
Σ SQDG		3.84	0.49	13%

^a Average molecular weight.





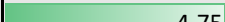






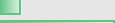













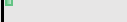
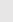

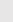

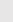
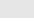



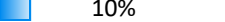
^b nmol mg⁻¹ of dry weight.

^c The intensities of the two product ions associated with the fatty acyl chain were equivalent, and thus the preferential regiochemistry was undetermined in this case.

Polar lipid fatty acid determination from polar lipid molecular species

As illustrated in Equations 1 and 2, it is possible to deduce the number of moles of each fatty acid, knowing the number of moles of each molecular species for the combination of the whole polar lipid classes. By summing for example all the 16:1, 18:3 or 20:5 from the various polar lipids they belongs to, a profile of fatty acids from polar lipids (PLFAs) can be estimated for the two microalgae (Table 3).

Table 3. Equivalent of PLFA amounts from the polar lipidome of *N. palea* (left) and *S. costatus* (right), $n=5$ for each microalgae.

PLFA (% mol)	Diatom			Green algae		
	Mean (nmol.mg ⁻¹)	SD	%RSD	Mean (nmol.mg ⁻¹)	SD	%RSD
14:0	 0.13	0.06	46%	 N.D	N.D	N.D
16:0	 1.16	0.38	33%	 1.76	0.06	4%
16:1	 4.75	1.78	38%	 0.94	0.09	9%
16:2	 0.19	0.10	50%	 0.32	0.03	10%
16:3	 0.00	N.D	N.D	 0.65	0.06	12%
16:4	 0.00	N.D	N.D	 3.39	0.10	12%
18:0	 0.00	N.D	N.D	 N.D	N.D	N.D
18:1	 0.85	0.30	35%	 1.51	0.13	9%
18:2	 0.00	N.D	N.D	 1.56	0.16	10%
18:3	 0.00	N.D	N.D	 6.70	0.20	5%
18:4	 0.00	N.D	N.D	 0.01	0.00	4%
20:0	 0.15	0.06	38%	 N.D	N.D	N.D
20:1	 0.00	N.D	N.D	 N.D	N.D	N.D
20:2	 2.66	1.42	53%	 N.D	N.D	N.D
20:5	 3.59	1.76	49%	 N.D	N.D	N.D
22:6	 0.11	0.01	11%	 N.D	N.D	N.D
Σ SFA	 12%	1%	N.D	 10%	0.00	N.D
Σ MUFA	 43%	2%	N.D	 15%	0.01	N.D
Σ PUFA	 45%	2%	N.D	 75%	0.01	N.D
PUFA/(SFA+MUFA)	0.83	0.05	6%	3.01	0.32	11%

It was thus obtained two very different profiles, in which we find respectively the predominance of 16:1, 20:2 and 20:5, then to a lesser extent 16:0 and 18:1 for the diatom (*N. palea*), and a majority of 16:4 and 18:3, followed by 16:0, 18:1 and 18:2 for the green algae (*S. costatus*). Zhang et al.⁴⁵ showed that six different diatom strains exhibited fatty acid compositions typical of the class *Bacillariophyceae*, with a majority of 14:0, 16:0, 16:1, and 20:5. Among these strains, the authors identified *N. palea* HB170, which showed a fatty acid composition in agreement with our observations, although in our study we focused on polar lipids while Zhang et al. determined the total fatty acid content or that derived from triglycerides alone.

Regarding green algae, Sato, et al.⁴⁶ previously reported the occurrence of pinolenic acid (18:3 n -6) and coniferonic acid (18:4 n -3) in the case of *Chlamydomonas reinhardtii*. In our case, we do observe for *S. costatus* the presence of 18:3, potentially corresponding to pinolenic acid described earlier, but 18:4, which could be associated with coniferonic acid, was barely detected. Moreover, 18:3 may also correspond to α -linolenic acid⁴⁷. As for 16:4 observed in our green algae extracts, which is typically derived from galactolipids as reported by Kumari, et al.⁴⁸, it may correspond to an unusual n -3 PUFA also reported with *Chlamydomonas reinhardtii*. The majority of diatom species (or *Bacillariophyta*) investigated in literature^{17, 49} synthesize glycolipids with a prokaryotic structure, confirming our previous observations. The characteristic fatty acids of diatoms from these glycolipids are 14:0, 16:0, 16:1, and 20:5 n -3 or eicosapentaenoic acid, whereas 16:2, 16:3, 16:4 18:0, 18:1, 18:2 or 18:3 fatty acids are in general lower or even absent⁵⁰. The desaturation degree and the amount of C16 fatty acids vary in the different diatom species. Moreover, 16:3 and 16:4 are only present in glycolipids, when occurring, while 20:5 is found in all lipids, but restricted to sn -1 position in glycolipids^{21, 51-52}, which was consistent with our observations for both MGDG and DGDG (Table 1). To conclude this section, eicosadienoic acid (20:2 n -6) is a long chain PUFA less frequently observed than eicosapentaenoic in diatoms⁵³. This fatty acid can

be obtained from $\Delta 9$ elongation of linoleic acid, and could be considered here as a likely specific marker of *N. palea*.

Acknowledgments

The authors would like to thank for technical Sylvia Moreira, Gwilherm Jan and Jacky Vedrenne for laboratory assistance regarding microalgae cultures. The authors thank as well the Aquatic Vegetation Pole of the ISC XPO (<https://doi.org/10.17180/BREY-MR38>) of the UR EABX for providing the laboratories and equipment necessary to perform the analyses in this study.

Conflict of interest

The authors declared no competing interest.

Funding

This study has been carried out with financial support from the French National Research Agency (ANR) in the frame of the Investments for the future Programme, within the Cluster of Excellence COTE (ANR-10-LABX-45).

References

1. Taipale, S.; Strandberg, U.; Peltomaa, E.; Galloway, A. W. E.; Ojala, A.; Brett, M. T., Fatty acid composition as biomarkers of freshwater microalgae: analysis of 37 strains of microalgae in 22 genera and in seven classes. *Aquat. Microb. Ecol.* **2013**, *71*, 165–178.
2. Brett, M. T.; Müller-Navarra, D. C., The role of highly unsaturated fatty acids in aquatic foodweb processes. *Freshw. Biol.* **1997**, *38*, 483–499.
3. Kelly, J. R.; Scheibling, R. E., Fatty acids as dietary tracers in benthic food webs. *Mar. Ecol. Prog. Ser.* **2012**, *446*, 1–22.
4. Arts, M. T.; Ackman, R. G.; Holub, B. J., Essential fatty acids' in aquatic ecosystems: a crucial link between diet and human health and evolution. *Can J Fish Aquat Sci* **2001**, *58*, 122–137.
5. Demailly, F.; Elfeky, I.; Malbezin, L.; Le Guédard, M.; Eon, M.; Bessoule, J.-J.; Feurtet-Mazel, A.; Delmas, F.; Mazzella, N.; Gonzalez, P.; Morin, S., Impact of diuron and S-metolachlor on the freshwater diatom *Gomphonema gracile*: Complementarity between fatty acid profiles and different kinds of ecotoxicological impact-endpoints. *Science of The Total Environment* **2019**, *688*, 960-969.
6. Mizusawa, N.; Wada, H., The role of lipids in photosystem II. *Biochimica et Biophysica Acta (BBA) - Bioenergetics* **2012**, *1817* (1), 194-208.
7. Da Costa, E.; Silva, J.; Mendonça, S. H.; Abreu, M. H.; Domingues, M. R., Lipidomic Approaches towards Deciphering Glycolipids from Microalgae as a Reservoir of Bioactive Lipids. *Marine Drugs* **2016**, *14* (5), 101.
8. Guschina, I. A.; Harwood, J. L., Lipids and lipid metabolism in eukaryotic algae. *Progress in Lipid Research* **2006**, *45* (2), 160-186.
9. Cutignano, A.; Luongo, E.; Nuzzo, G.; Pagano, D.; Manzo, E.; Sardo, A.; Fontana, A., Profiling of complex lipids in marine microalgae by UHPLC/tandem mass spectrometry. *Algal Research* **2016**, *17*, 348-358.
10. Li, X.; He, Q.; Hou, H.; Zhang, S.; Zhang, X.; Zhang, Y.; Wang, X.; Han, L.; Liu, K., Targeted lipidomics profiling of marine phospholipids from different resources by UPLC-Q-Exactive Orbitrap/MS approach. *Journal of Chromatography B* **2018**, *1096*, 107-112.
11. Rimet, F.; Chardon, C.; Lainé, L.; Bouchez, A.; Domaizon, I.; Guillard, J.; Jacquet, S., "Thonon Culture Collection -TCC- a freshwater microalgae collection", <https://doi.org/10.15454/UQEMVW>, Portail Data Inra, V1. **2018**.
12. Dauta, A., Conditions de développement du phytoplancton. Etude comparative du comportement de huit espèces en culture. II: Rôle des nutriments : assimilation et stockage intracellulaire. *Annales De Limnologie-International Journal of Limnology* **1982**, *18*, 263-292.
13. Matyash, V.; Liebisch, G.; Kurzchalia, T. V.; Shevchenko, A.; Schwudke, D., Lipid extraction by methyl-tert-butyl ether for high-throughput lipidomics. *Journal of Lipid Research* **2008**, *49* (5), 1137-1146.
14. Mazzella, N.; Moreira, A.; Eon, M.; Médina, A.; Millan-Navarro, D.; Creusot, N., Hydrophilic interaction liquid chromatography coupled with tandem mass spectrometry method for quantification of five phospholipid classes in various matrices. *MethodsX In press*.
15. Li-Beisson, Y.; Thelen, J. J.; Fedosejevs, E.; Harwood, J. L., The lipid biochemistry of eukaryotic algae. *Progress in Lipid Research* **2019**, *74*, 31-68.
16. Zulu, N. N.; Zienkiewicz, K.; Vollheyde, K.; Feussner, I., Current trends to comprehend lipid metabolism in diatoms. *Progress in Lipid Research* **2018**, *70*, 1-16.
17. Alonso, D. L.; Belarbi, E.-H.; Rodríguez-Ruiz, J.; Segura, C. I.; Giménez, A., Acyl lipids of three microalgae. *Phytochemistry* **1998**, *47* (8), 1473-1481.
18. Li, L.; Chang, M.; Tao, G.; Wang, X.; Liu, Y.; Liu, R.; Jin, Q.; Wang, X., Analysis of phospholipids in *Schizochytrium* sp. S31 by using UPLC-Q-TOF-MS. *Analytical Methods* **2016**, *8* (4), 763-770.
19. Jouhet, J.; Lupette, J.; Clerc, O.; Magneschi, L.; Bedhomme, M.; Collin, S.; Roy, S.; Maréchal, E.; Rébeillé, F., LC-MS/MS versus TLC plus GC methods: Consistency of

glycerolipid and fatty acid profiles in microalgae and higher plant cells and effect of a nitrogen starvation. *PLOS ONE* **2017**, *12* (8), e0182423.

20. Coniglio, D.; Bianco, M.; Ventura, G.; Calvano, C. D.; Losito, I.; Cataldi, T. R. I., Lipidomics of the Edible Brown Alga Wakame (*Undaria pinnatifida*) by Liquid Chromatography Coupled to Electrospray Ionization and Tandem Mass Spectrometry. *Molecules* **2021**, *26* (15), 4480.

21. Yongmanitchai, W.; Ward, O. P., Positional distribution of fatty acids, and molecular species of polar lipids, in the diatom *Phaeodactylum tricornutum*. *Journal of general microbiology* **1993**, *139* (3), 465-72.

22. Degraeve-Guilbault, C.; Bréhélin, C.; Haslam, R.; Sayanova, O.; Marie-Luce, G.; Jouhet, J.; Corellou, F., Glycerolipid Characterization and Nutrient Deprivation-Associated Changes in the Green Picoalga *Ostreococcus tauri*. *Plant Physiology* **2017**, *173* (4), 2060.

23. Hsu, F.-F.; Turk, J., Electrospray ionization with low-energy collisionally activated dissociation tandem mass spectrometry of glycerophospholipids: Mechanisms of fragmentation and structural characterization. *Journal of Chromatography B* **2009**, *877* (26), 2673-2695.

24. Yingbo, Z.; Ximan, K.; Yajuan, W.; Huajun, S.; Shujuan, J., Comprehensive analysis of phospholipids and glycerol glycolipids in green pepper by ultra-performance liquid chromatography/quadrupole time-of-flight mass spectrometry. *Rapid Communications in Mass Spectrometry* **2021**, *35* (18), e9146.

25. Tatituri, R. V. V.; Brenner, M. B.; Turk, J.; Hsu, F.-F., Structural elucidation of diglycosyl diacylglycerol and monoglycosyl diacylglycerol from *Streptococcus pneumoniae* by multiple-stage linear ion-trap mass spectrometry with electrospray ionization. *Journal of Mass Spectrometry* **2012**, *47* (1), 115-123.

26. Herrero, M.; Vicente, M. J.; Cifuentes, A.; Ibáñez, E., Characterization by high-performance liquid chromatography/electrospray ionization quadrupole time-of-flight mass spectrometry of the lipid fraction of *Spirulina platensis* pressurized ethanol extract. *Rapid*

communications in mass spectrometry : RCM **2007**, *21* (11), 1729-38.

27. Mazzella, N.; Molinet, J.; Syakti, A. D.; Dodi, A.; Bertrand, J.-C.; Doumenq, P., Use of electrospray ionization mass spectrometry for profiling of crude oil effects on the phospholipid molecular species of two marine bacteria. *Rapid Communications in Mass Spectrometry* **2005**, *19* (23), 3579-3588.

28. Fournier, F.; Remaud, B.; Blasco, T.; Tabet, J. C., Ion-dipole complex formation from deprotonated phenol fatty acid esters evidenced by using gas-phase labeling combined with tandem mass spectrometry. *Journal of the American Society for Mass Spectrometry* **1993**, *4* (4), 343-351.

29. Mazzella, N.; Molinet, J.; Syakti, A. D.; Dodi, A.; Doumenq, P.; Artaud, J.; Bertrand, J.-C., Bacterial phospholipid molecular species analysis by ion-pair reversed-phase HPLC/ESI/MS. *Journal of Lipid Research* **2004**, *45* (7), 1355-1363.

30. Hsu, F.-F.; Turk, J., Studies on phosphatidylglycerol with triple quadrupole tandem mass spectrometry with electrospray ionization: Fragmentation processes and structural characterization. *Journal of the American Society for Mass Spectrometry* **2001**, *12* (9), 1036-1043.

31. Pi, J.; Wu, X.; Feng, Y., Fragmentation patterns of five types of phospholipids by ultra-high-performance liquid chromatography electrospray ionization quadrupole time-of-flight tandem mass spectrometry. *Analytical Methods* **2016**, *8* (6), 1319-1332.

32. Huang, Q.; Lei, H.; Dong, M.; Tang, H.; Wang, Y., Quantitative analysis of 10 classes of phospholipids by ultrahigh-performance liquid chromatography tandem triple-quadrupole mass spectrometry. *Analyst* **2019**, *144* (13), 3980-3987.

33. Hsu, F.-F.; Turk, J., Charge-remote and charge-driven fragmentation processes in diacyl glycerophosphoethanolamine upon low-energy collisional activation: a mechanistic proposal. *Journal of the American Society for Mass Spectrometry* **2000**, *11* (10), 892-899.

34. Mazzella, N.; Molinet, J.; Syakti, A. D.; Bertrand, J.-C.; Doumenq, P., Assessment of the effects of hydrocarbon contamination on the

- sedimentary bacterial communities and determination of the polar lipid fraction purity: Relevance of intact phospholipid analysis. *Marine Chemistry* **2007**, *103* (3), 304-317.
35. Zulfiqar, S.; Sharif, S.; Saeed, M.; Tahir, A., *Role of Carotenoids in Photosynthesis. In: Photosynthesis. Advances in Photosynthesis and Respiration, vol 10.* . Springer, Dordrecht: 2003.
 36. Giroud, C.; Gerber, A.; Eichenberger, W., Lipids of *Chlamydomonas reinhardtii*. Analysis of Molecular Species and Intracellular Site(s) of Biosynthesis. *Plant and Cell Physiology* **1988**, *29* (4), 587-595.
 37. Sanina, N. M.; Goncharova, S. N.; Kostetsky, E. Y., Fatty acid composition of individual polar lipid classes from marine macrophytes. *Phytochemistry* **2004**, *65* (6), 721-30.
 38. Choi, K.; Nakhost, Z.; Bárzana, E.; Karel, M., Lipid content and fatty acid composition of green algae *Scenedesmus obliquus* grown in a constant cell density apparatus. *Food biotechnology* **1987**, *1*, 117-28.
 39. Block, M. A.; Dorne, A. J.; Joyard, J.; Douce, R., Preparation and characterization of membrane fractions enriched in outer and inner envelope membranes from spinach chloroplasts. II. Biochemical characterization. *The Journal of biological chemistry* **1983**, *258* (21), 13281-6.
 40. Demé, B.; Cataye, C.; Block, M. A.; Maréchal, E.; Jouhet, J., Contribution of galactoglycerolipids to the 3-dimensional architecture of thylakoids. *FASEB journal : official publication of the Federation of American Societies for Experimental Biology* **2014**, *28* (8), 3373-83.
 41. Wada, H.; Murata, N., The essential role of phosphatidylglycerol in photosynthesis. *Photosynthesis research* **2007**, *92*, 205-15.
 42. Apostolova, E. L.; Domonkos, I.; Dobrikova, A. G.; Sallai, A.; Bogos, B.; Wada, H.; Gombos, Z.; Taneva, S. G., Effect of phosphatidylglycerol depletion on the surface electric properties and the fluorescence emission of thylakoid membranes. *Journal of Photochemistry and Photobiology B: Biology* **2008**, *91* (1), 51-57.
 43. Vyssotski, M.; Lagutin, K.; MacKenzie, A.; Mitchell, K.; Scott, D., Phospholipids of New Zealand Edible Brown Algae. *Lipids* **2017**, *52* (7), 629-639.
 44. Berge, J.-P.; Gouygou, J.-P.; Dubacq, J.-P.; Durand, P., Reassessment of lipid composition of the diatom, *Skeletonema costatum*. *Phytochemistry* **1995**, *39* (5), 1017-1021.
 45. Lingxiang, Z.; It; sup; gt; It; sup; gt; Fan, H.; It; sup; gt; It; sup; gt; Xiu, W.; It; sup; gt; It; sup; gt; Yufang, P.; It; sup; gt; It; sup; gt; Hanhua, H.; It; sup; gt; *; It; sup; gt; Screening of High Temperature-Tolerant Oleaginous Diatoms. *J. Microbiol. Biotechnol.* **2020**, *30* (7), 1072-1081.
 46. Sato, N.; Sonoike, K.; Tsuzuk, M.; Kawaguchi, A., Impaired Photosystem II in a Mutant of *Chlamydomonas Reinhardtii* Defective in Sulfoquinovosyl Diacylglycerol. *European Journal of Biochemistry* **1995**, *234* (1), 16-23.
 47. Kajikawa, M.; Yamato, K. T.; Kohzu, Y.; Shoji, S.; Matsui, K.; Tanaka, Y.; Sakai, Y.; Fukuzawa, H., A front-end desaturase from *Chlamydomonas reinhardtii* produces pinolenic and coniferonic acids by omega13 desaturation in methylotrophic yeast and tobacco. *Plant & cell physiology* **2006**, *47* (1), 64-73.
 48. Kumari, P.; Bijo, A. J.; Mantri, V. A.; Reddy, C. R.; Jha, B., Fatty acid profiling of tropical marine macroalgae: an analysis from chemotaxonomic and nutritional perspectives. *Phytochemistry* **2013**, *86*, 44-56.
 49. Abida, H.; Dolch, L. J.; Meï, C.; Villanova, V.; Conte, M.; Block, M. A.; Finazzi, G.; Bastien, O.; Tirichine, L.; Bowler, C.; Rébeillé, F.; Petroutsos, D.; Jouhet, J.; Maréchal, E., Membrane glycerolipid remodeling triggered by nitrogen and phosphorus starvation in *Phaeodactylum tricornutum*. *Plant Physiol* **2015**, *167* (1), 118-36.
 50. Lang, I.; Hodac, L.; Friedl, T.; Feussner, I., Fatty acid profiles and their distribution patterns in microalgae: a comprehensive analysis of more than 2000 strains from the SAG culture collection. *BMC Plant Biol* **2011**, *11*, 124-124.
 51. D'Ippolito, G.; Sardo, A.; Paris, D.; Vella, F. M.; Adelfi, M. G.; Botte, P.; Gallo, C.; Fontana, A., Potential of lipid metabolism in marine diatoms for biofuel production. *Biotechnol Biofuels* **2015**, *8*, 28.
 52. Xu, J.; Chen, D.; Yan, X.; Chen, J.; Zhou, C., Global characterization of the

photosynthetic glycerolipids from a marine diatom *Stephanodiscus* sp. by ultra performance liquid chromatography coupled with electrospray ionization-quadrupole-time of flight mass spectrometry. *Analytica Chimica Acta* **2010**, 663 (1), 60-68.

53. Sayanova, O.; Mimouni, V.; Ulmann, L.; Morant-Manceau, A.; Pasquet, V.; Schoefs, B.;

Napier, J. A., Modulation of lipid biosynthesis by stress in diatoms. *Philosophical transactions of the Royal Society of London. Series B, Biological sciences* **2017**, 372 (1728).

2 **Captions for supplementary information**

3

4 Table S 1. HPLC gradients for phospholipid and glycolipid analysis.

5

6 Table S 2. Limits of quantification estimates and retentions times.

7

8 Table S 3. ESI and MS/MS parameters for phospholipids and glycolipids.

9 Table S 4. MRM transitions.

10